

Towards Privacy Protection by Generating Adversarial Identity Masks

Xiao Yang Yinpeng Dong Tianyu Pang Jun Zhu Hang Su

Dept. of Comp. Sci. and Tech., BNRist Center, State Key Lab for Intell. Tech. & Sys,
Institute for AI, THBI Lab, Tsinghua University, Beijing, 100084, China
{yangxiao19, dyp17, pty17}@mails.tsinghua.edu.cn,
{dcszj, suhangss}@mail.tsinghua.edu.cn

Abstract. As billions of personal data such as photos are shared through social media and network, the privacy and security of data have drawn an increasing attention. Several attempts have been made to alleviate the leakage of identity information with the aid of image obfuscation techniques. However, most of the present results are either perceptually unsatisfactory or ineffective against real-world recognition systems. In this paper, we argue that an algorithm for privacy protection must block the ability of automatic inference of the identity and at the same time, make the resultant image natural from the users’ point of view. To achieve this, we propose a targeted identity-protection iterative method (TIP-IM), which can generate natural face images by adding adversarial identity masks to conceal ones’ identity against a recognition system. Extensive experiments on various state-of-the-art face recognition models demonstrate the effectiveness of our proposed method on alleviating the identity leakage of face images, without sacrificing the visual quality of the protected images.

1 Introduction

The blooming development of social media and network has brought a huge amount of personal data (e.g., photos) shared publicly. With the growing ubiquity of deep neural networks, these techniques dramatically improve the capabilities for an advanced face recognition system to deal with personal data [25,18,30,3], but as a byproduct, also increase the potential risks for privacy leakage of personal information. For example, an unauthorized third party may scramble and identify the shared photos on social media (e.g., Twitter, Facebook, LinkedIn, etc.) without the permission of their owners, resulting in cybercasting [16]. Therefore, it is imperative to provide users an effective way to protect their private information from being unconsciously identified and exposed by the excessive unauthorized systems, without affecting users’ experience

The past years have witnessed the progress for privacy protection in both the security and computer vision communities. Among the existing techniques, the most studied category is based on image obfuscation. Conventional obfuscation techniques [32], such as blurring, pixelation, darkening, and occlusion, are maybe either perceptually satisfactory or effective against recognition systems [21,19].

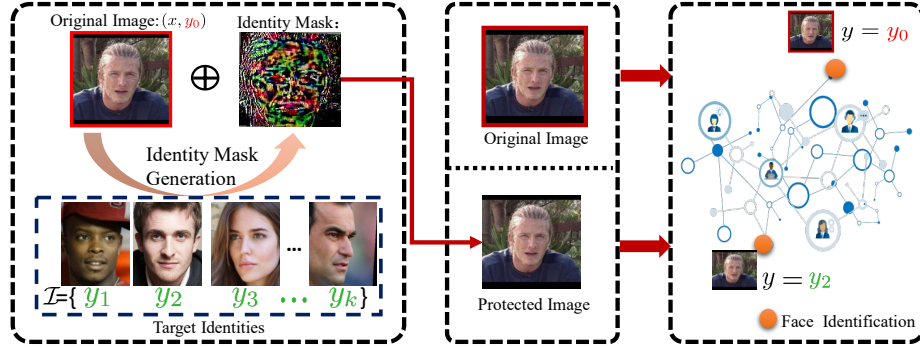


Fig. 1. An illustrative example of targeted identity protection. When users share photos on social media (e.g., Twitter, Facebook, LinkedIn, *etc.*), unauthorized applications could scramble their identities by searching for private websites or social media profiles based on face recognition systems, resulting in the privacy leakage of personal information (e.g., name, phone number, address) tied to identity profiles. Therefore, we provide an effective tool that allows users to conceal the identity information while not affect the visual quality of their photos. Once exposed to the unauthorized face systems, an image protected by the identity mask can conceal the corresponding identity by misleading the malicious systems to predict it as a wrong authorized or virtual target, which could be provided by the service providers.

The recent advance in generative adversarial networks (GANs) [8] provides an appealing way to generate more realistic images for obfuscation [27,28,33,17,7]. However, these methods are not problemless. *First*, the generated obfuscated images have significantly different visual appearances compared with the original images due to the exaggeration and suppression of some discriminative features, and thus fail to preserve utility for users. *Second*, they occasionally generate unnatural output images [28], which exhibit undesirable artifacts. *Third*, they are only used to hide the personal identity against automatic recognition systems, without the capability in specifying the target output identity. Fourth, compared to model-based obfuscation method like GAN, our method is algorithm-based, which is off-the-shelf for different data distributions.

Recent researches have found that face recognition systems are vulnerable to adversarial examples [29,9,4,26,5], which can significantly change the outputs of a system by adding small perturbations. Although they pose security threats to face recognition systems, it is an appealing way to apply an adversarial perturbation to conceal one’s identity, even under a more strict constraint of impersonating some authorized or generated face images when available (e.g., given by the social media services). It provides a possible solution to specify the output, which may avoid an invasion of privacy to other persons if the resultant image is recognized as an arbitrary identity. It should be noted that although the adversarial perturbations generated by the existing methods have a small intensity change (e.g., 12 or 16 for each pixel in $[0, 255]$), they may still sacrifice the visual quality with artifacts [35], as illustrated in Fig. 2. Moreover, the current adversarial attacks are mainly dependent on either the *white-box* control of the target system [26,22] or the tremendous number of *model queries* [5], which are

impractical in real-world scenarios (e.g., unauthorized face recognition systems on social media) for privacy protection.

In this paper, we propose a practical **targeted identity-protection attack** setting to alleviate the identity leakage of personal photos in real-world social media. We focus on face identification in particular, the goal of which is to identify a real face image in a unknown gallery identity set (see in Sec. 3), since it can be adopted by unauthorized applications for recognizing the identity information of users. As stated in Fig. 1, *privacy protection* is to block the ability of automatic inference on malicious applications, making them predict a wrong authorized or virtual target by the service providers. Compared with the conventional adversarial attack settings (e.g., dodging, impersonation), the proposed targeted identity-protection setting is different yet more challenging. In general, little is known about the face identification system and no direct query access is possible. Therefore, we need to generate adversarial examples against a surrogate white-box model with the purpose of deceiving a black-box face identification system. Moreover, we aim to not affect the user experience when users share the protected photos on social media, meanwhile conceal their identities from unauthorized identification systems. Thus, the adversarial examples should also be visually natural from the corresponding original ones for human eyes, otherwise undesirable artifacts may be introduced.

To address the aforementioned challenges, we propose a **targeted identity-protection iterative method** (TIP-IM) for privacy protection against black-box face identification systems. The proposed method generates adversarial identity masks that are both transferable and imperceptible. A good transferability can assure to effectively deceive other black-box face identification systems, meanwhile the imperceptibility means that a photo manipulated by an adversarial identity mask is visually natural for the human observers. Specifically, to ensure the generated adversarial images are not arbitrarily misclassified as other identities, we randomly choose a set of face images from a celebrity dataset collected from the internet as the specified attack targets in our experiments¹. Our method is capable of finding a potential target from the chosen set of face images with multiple identities via an optimization process, which makes the identity protection easier compared with using only one single target.

We apply the proposed method to measure the success rate of identity protection against the current state-of-the-art face models, including SpheroFace [18], CosFace [30], FaceNet [25], ArcFace [3], MobileFace [2], and ResNet50 [11]. Extensive experiments conducted on the Labeled Face in the Wild (LFW) [12] dataset and MegaFace Challenge [14] demonstrate its effectiveness under the above setting. Our main contributions are summarized as

- We establish a practical identity protection setting to simulate identification systems on the social media, which can provide a general understanding for the current privacy protection.

¹ We choose face images from the Internet only for experimental illustration. And our algorithm is applicable for any authorized or generated target set of face images.

	Evasion [32]	PP-GAN [33]	Inpainting [27]	Replacement [28]	Eyeglasses [26]	Evolutionary [5]	GAMAN [22]	Ours
Unknown gallery set	No	No	No	No	No	Yes	No	Yes
Target identity	No	No	No	No	Yes	Yes	Yes	Yes
Black-box model	Yes	Yes	Yes	Yes	No	<i>Yes (Queries)</i>	No	Yes
Natural outputs	No	Yes	Yes	Yes	No	No	No	Yes
Same faces	<i>Partially</i>	<i>Partially</i>	No	No	Yes	Yes	Yes	Yes

Table 1. A comparison between different methods in terms of the unknown gallery set, targeted misclassification of the output faces, black-box face models, natural output faces, and whether the output faces are recognized as the same identities as the original ones for human observers. Note that [5] considers the black-box face models with queries, but our method does not rely on such information.

- We propose a targeted identity-protection iterative method (TIP-IM), which enables to generate a natural protected image by adding an adversarial identity mask, providing a user a possible solution to automatically conceal one’s identity without sacrificing the visual quality of photos significantly.
- Extensive experiments based on the state-of-the-art face recognition models demonstrate the effectiveness of the proposed method on alleviating identity leakage of personal photos.

2 Related Work

In this section, we review related work on face privacy protection. We provide a comprehensive comparison between the previous methods and ours in Table 1.

Privacy protection of face images. Several works have been developed to protect private identity information in personal photos against face or person recognition systems. Earlier works [32,24] study the performance of these systems under various simple image obfuscation methods, such as blurring, pixelation, darkening, occlusion, etc. These methods have been shown to be ineffective against the current recognition systems [21,19], since they can adapt to the obfuscation patterns. More sophisticated techniques have been proposed thereafter. For example, generative adversarial networks (GANs) [8] provide a useful way to synthesize realistic images on the data distribution for image obfuscation [33]. In [27], the obfuscated images are generated by head in-painting conditioned on the detected face landmarks. A following work [28] combines a parametric face model with a GAN model for obtaining better performance. A recent work [17] extends the previous works by balancing the utility and privacy of the generated images. Privacy protection is also considered on videos [7]. However, the aforementioned image obfuscation methods often change the visual appearances of face images and even lead to unnatural outputs, limiting their utility for users. Moreover, they cannot specify the target identities to be wrongly classified by the face recognition models, which in some cases may violate the privacy of other irrelevant persons. In this paper, we study adversarial examples as a powerful obfuscation method for privacy protection.

Adversarial attacks on face recognition. Deep neural networks are susceptible to adversarial examples [29,9,4], so are the face recognition models [26,5]. In previous works, the adversary can perform either *dodging* (i.e., recognized wrongly) or *impersonation* (i.e., recognized as a target identity) attacks, based on the *white-box* gradient information or the *black-box* model queries. A recent work [22] proposes to adopt adversarial examples for privacy protection from a game theory perspective. However, our work is significantly different from this previous work in three aspects. First, we consider the open-set face identification protocol [18] with an unknown gallery set, while [22] uses a closed-set scenario. Second, we focus on the black-box attack setting, while [22] assumes the white-box access to the target model. Third, we aim to generate natural adversarial examples, while [22] does not consider the naturalness of adversarial examples.

3 Proposed Attack Setting for Privacy Protection

Let $f(\mathbf{x}) : \mathcal{X} \rightarrow \mathbb{R}^d$ denote a face recognition model that extracts a fixed length feature representation in \mathbb{R}^d for an input face image $\mathbf{x} \in \mathcal{X} \subset \mathbb{R}^n$. Given the metric $\mathcal{D}_f(\mathbf{x}_1, \mathbf{x}_2) = \|f(\mathbf{x}_1) - f(\mathbf{x}_2)\|_2^2$ that measures the feature distance between two face images, face identification compares the distance between a probe image and a gallery set of face images $\mathcal{G} = \{\mathbf{x}_1^g, \dots, \mathbf{x}_m^g\}$, and returns the identity whose face image has the smallest feature distance with the probe image.

In this paper, we propose a novel yet practical attack setting called **targeted identity-protection attack** to protect personal privacy against face identification systems, as illustrated in Fig. 1. Specifically, to conceal the true identity y of a face image \mathbf{x}^{real} , we aim to generate an example \mathbf{x}^{adv} by adding an adversarial identity mask to \mathbf{x}^{real} , to make the face identification system predict it as a different authorized identity or virtual identity corresponding to a generated image. Rather than specifying a single target identity for generating the adversarial example, we manually choose an identity set $\mathcal{I} = \{y_1, \dots, y_k\}$, i.e., we allow the face identification system to recognize the adversarial example as arbitrary one of the target identities in \mathcal{I} rather than a single one, which makes identity protection easier to achieve due to the relaxed constraints.

Formally, let $\mathcal{G}_y = \{\mathbf{x} | \mathbf{x} \in \mathcal{G}, \mathcal{O}(\mathbf{x}) = y\}$ denote a subset of \mathcal{G} containing all face images belonging to the true identity y of \mathbf{x}^{real} , with \mathcal{O} being an oracle to give the ground-truth identity labels, and $\mathcal{G}_{\mathcal{I}} = \bigcup_{1 \leq i \leq k} \mathcal{G}_{y_i}$ denote the face images belonging to the target identities of \mathcal{I} in the gallery set \mathcal{G} . To conceal the identity of \mathbf{x}^{real} , the adversarial example \mathbf{x}^{adv} should satisfy the constraint as

$$\exists \mathbf{x}' \in \mathcal{G}_{\mathcal{I}}, \forall \mathbf{x} \in \mathcal{G}_y : \mathcal{D}_f(\mathbf{x}^{adv}, \mathbf{x}) > \mathcal{D}_f(\mathbf{x}^{adv}, \mathbf{x}'). \quad (1)$$

It ensures that the feature distance between the generated adversarial image \mathbf{x}^{adv} and a target identity's image \mathbf{x}' in $\mathcal{G}_{\mathcal{I}}$ is smaller than that between \mathbf{x}^{adv} and any image belonging to the true identity y in \mathcal{G}_y .

The proposed attack setting is designed for privacy protection of face images, and is significantly different from the previous studied dodging and impersonation attacks [26,22,5], in the following three aspects.



Fig. 2. Illustration of different perturbations under the l_∞ norm.

Naturalness. To make the adversarial example indistinguishable from the corresponding original one, a common practice is to restrict the ℓ_p ($p = 2, \infty$, etc.) norm between the adversarial and original examples, as $\|\mathbf{x}^{adv} - \mathbf{x}^{real}\|_p \leq \epsilon$. However, the perturbation under the ℓ_p norm is still perceptible [35], as also illustrated in Fig. 2. Therefore, we further require that the adversarial example should look natural besides the constraint of the ℓ_p norm bound, to make it really imperceptible for human eyes, which is not considered in previous works. We use an objective function to promote the naturalness of the adversarial example, which will be specified in Sec. 4.1.

Unawareness of gallery set. For a real-world face identification system, we have no knowledge of its gallery set \mathcal{G} , meaning that we are not able to solve Eq. (1) directly, while previous works assume the availability of the gallery set or a closed-set protocol (i.e., no gallery set). To address this issue, we use substitute face images for optimization. In particular, we collect an image set $\hat{\mathcal{G}}_{\mathcal{I}}$ containing face images that belong to the target identities of \mathcal{I} as a surrogate for $\mathcal{G}_{\mathcal{I}}$; and use $\{\mathbf{x}^{real}\}$ directly instead of \mathcal{G}_y . The rationality of using substitute images is that face representations of one identity are similar, and thus the representation of an adversarial example optimized to be similar to the substitutes can also be close to images belonging to the same target identity in the gallery set.

Black-box attack. In practice, we are also unaware of the face identification model, include its architecture, parameters, and gradients. Previous methods rely on either the white-box access to the target model or the tremendous number of queries, which are impractical in real-world scenarios for privacy protection. Therefore, we adopt a surrogate white-box model against which the adversarial examples are generated, with the purpose of attacking black-box models based on the transferability of adversarial example [23, 4].

In summary, our setting is designed to simulate the real-world scenarios with minimum assumptions of the target face identification system, which is also more challenging than previously studied settings.

4 Methodology

To achieve the above requirements, we propose a **targeted identity-protection iterative method** (TIP-IM) to generate adversarial examples in this section.

4.1 Problem Formulation

To generate an adversarial example \mathbf{x}^{adv} that is both effective for obfuscation against face identification systems and visually natural for human eyes, we for-

malize the objective of targeted privacy-protection attack as

$$\min_{\mathbf{x}^{adv}} \left\{ \min_{\mathbf{x}' \in \hat{\mathcal{G}}_{\mathcal{I}}} \mathcal{J}_{iden}(\mathbf{x}', \mathbf{x}^{adv}) + \gamma \cdot \mathcal{J}_{nat}(\mathbf{x}^{adv}) \right\}, \text{ s.t. } \|\mathbf{x}^{adv} - \mathbf{x}^{real}\|_p \leq \epsilon, \quad (2)$$

where \mathcal{J}_{iden} is an identification loss that makes the face identification model recognize \mathbf{x}^{adv} as the target identity of \mathbf{x}' , \mathcal{J}_{nat} promotes \mathbf{x}^{adv} to look natural, and γ is a hyperparameter to balance these two losses. We also restrict the ℓ_p norm of the adversarial perturbation to be smaller than a constant ϵ . Note that for the unawareness of gallery set, we use the substitute face images $\hat{\mathcal{G}}_{\mathcal{I}}$ in our objective (2); for the black-box model, we generate an adversarial example \mathbf{x}^{adv} against a surrogate white-box model with the purpose of fooling the black-box model based on the transferability. Thus the requirements in the proposed targeted identity-protection attack can be fulfilled by solving Eq. (2).

The inner minimization $\min_{\mathbf{x}' \in \hat{\mathcal{G}}_{\mathcal{I}}} \mathcal{J}_{iden}$ of Eq. (2) aims to find the best target image in $\hat{\mathcal{G}}_{\mathcal{I}}$ such that the identification loss is minimized w.r.t. \mathbf{x}' . We define \mathcal{J}_{iden} as

$$\mathcal{J}_{iden}(\mathbf{x}', \mathbf{x}^{adv}) = \mathcal{D}_f(\mathbf{x}^{adv}, \mathbf{x}') - \mathcal{D}_f(\mathbf{x}^{adv}, \mathbf{x}^{real}). \quad (3)$$

By minimizing \mathcal{J}_{iden} as in Eq. (2), we actually minimize the feature distance between the adversarial example \mathbf{x}^{adv} and a face image \mathbf{x}' in $\hat{\mathcal{G}}_{\mathcal{I}}$, while maximize the feature distance between the adversarial and original images. Thus the inner minimization of Eq. (2) corresponds to finding $\mathbf{x}' \in \hat{\mathcal{G}}_{\mathcal{I}}$ such that the adversarial example \mathbf{x}^{adv} has the smallest distance to \mathbf{x}' in the feature space.

Although the perturbation is somewhat small due to the ℓ_p norm constraint in Eq. (2), it can be still perceptible and not natural for human eyes, as shown in Fig. 2. Therefore, we add a loss \mathcal{J}_{nat} into our objective to explicitly encourage the naturalness of the generated adversarial example. In this paper, we adopt the *maximum mean discrepancy* (MMD) [1] as \mathcal{J}_{nat} , because it is an effective non-parametric and differentiable metric capable of comparing two data distributions and evaluating the imperceptibility of the generated images. In our case, given two sets of data $\mathbf{X}^{adv} = \{\mathbf{x}_1^{adv}, \dots, \mathbf{x}_N^{adv}\}$ and $\mathbf{X}^{real} = \{\mathbf{x}_1^{real}, \dots, \mathbf{x}_N^{real}\}$ comprised of N adversarial and N real examples, MMD calculates their discrepancy by

$$\text{MMD}(\mathbf{X}^{adv}, \mathbf{X}^{real}) = \left\| \frac{1}{N} \sum_{i=1}^N \phi(\mathbf{x}_i^{adv}) - \frac{1}{N} \sum_{j=1}^N \phi(\mathbf{x}_j^{real}) \right\|_{\mathcal{H}}^2, \quad (4)$$

where $\phi(\cdot)$ maps the data to a reproducing kernel Hilbert space (RKHS) [1]. We adopt the same $\phi(\cdot)$ as in [1]. By minimizing MMD between the samples \mathbf{X}^{adv} from the adversarial distribution and the samples \mathbf{X}^{real} from the real data distribution, we can enforce \mathbf{X}^{adv} to lie on the real data distribution, meaning the adversarial examples in \mathbf{X}^{adv} will be as natural as real examples.

Since MMD is defined on the batches of images, we thus rewrite our objective (2) with a batch-based formulation² as

$$\begin{aligned} \min_{\mathbf{X}^{adv}} \left\{ \frac{1}{N} \sum_{i=1}^N \min_{\mathbf{x}'_i \in \hat{\mathcal{G}}_{\mathcal{I}}} \mathcal{J}_{iden}(\mathbf{x}'_i, \mathbf{x}_i^{adv}) + \gamma \cdot \text{MMD}(\mathbf{X}^{adv}, \mathbf{X}^{real}) \right\}, \\ \text{s.t. } \mathbf{x}_i^{adv} \in \mathbf{X}^{adv}, \mathbf{x}_i^{real} \in \mathbf{X}^{real} : \|\mathbf{x}_i^{adv} - \mathbf{x}_i^{real}\|_p \leq \epsilon. \end{aligned} \quad (5)$$

Considering the complexity of solving the bi-level optimization problem (5), we first introduce the iterative algorithm if the solution of inner minimization is given, and then detail how to solve the inner minimization.

4.2 Targeted Identity-Protection Iterative Method

When there is only one target face image in $\hat{\mathcal{G}}_{\mathcal{I}}$, we do not need to solve the inner minimization problem in Eq. (5), and the outer minimization problem can be effectively solved by various iterative gradient-based attack methods [15,4]. So in this section, we assume that we already obtain the solution of the inner problem, and introduce the *targeted identity-protection iterative method* (TIP-IM) to generate adversarial examples by solving the outer problem. We defer to Sec. 4.3 on how to solve the inner problem via a greedy insertion algorithm.

Given the solution \mathbf{x}'_i^* of the inner problem, We let $\mathcal{J}(\mathbf{X}^{adv})$ denote the overall loss function as

$$\mathcal{J}(\mathbf{X}^{adv}) = \frac{1}{N} \sum_{i=1}^N \mathcal{J}_{iden}(\mathbf{x}'_i^*, \mathbf{x}_i^{adv}) + \gamma \cdot \text{MMD}(\mathbf{X}^{adv}, \mathbf{X}^{real}). \quad (6)$$

We can therefore generate the batch of adversarial examples \mathbf{X}^{adv} by minimizing $\mathcal{J}(\mathbf{X}^{adv})$. Given the definitions of \mathcal{J}_{iden} and MMD in Eq. (3) and Eq. (4), $\mathcal{J}(\mathbf{X}^{adv})$ is a differentiable function w.r.t. \mathbf{X}^{adv} , and thus we can adopt iterative gradient-based attack methods to generate adversarial examples. In particular, we optimize \mathbf{X}^{adv} via

$$\mathbf{X}_{t+1}^{adv} = \Pi_{\{\mathbf{X}^{real}, \ell_p, \epsilon\}}(\mathbf{X}_t^{adv} - \alpha \cdot \text{Normalize}(\nabla_{\mathbf{X}} \mathcal{J}(\mathbf{X}_t^{adv}))), \quad (7)$$

where \mathbf{X}_t^{adv} is the batch of adversarial examples at the t -th iteration, α is the step size, Π is the projection function that projects the adversarial examples onto the ℓ_p norm bound, and $\text{Normalize}(\cdot)$ is used to normalize the gradient (e.g., a sign function under the ℓ_∞ norm bound or the ℓ_2 normalization under the ℓ_2 norm bound). We perform the iterative process for a total number of T iterations and get the final adversarial examples as \mathbf{X}_T^{adv} . To prevent adversarial examples from falling into local minima and improve their transferability for other black-box face identification models, we incorporate the momentum technique [4] into the iterative process.

² In case of there is only one single image or a small number of images, we can augment the images with multiple transformations to make up a large batch, with the results shown in Appendix C.

Algorithm 1: Inner Minimization via Greedy Insertion

Input: The attack objective function \mathcal{J}_{iden} from Eq. (3); a real face \mathbf{x}^{real} and a multi-identity face images $\hat{\mathcal{G}}_{\mathcal{I}}$; a feature representation function f ; a gain function G .

Input: The adversarial example \mathbf{x}^{adv} generated before the current iteration.

Output: The best target image \mathbf{x}^{*} in $\hat{\mathcal{G}}_{\mathcal{I}}$.

```

1  $g_{best} \leftarrow 0$ ;  $\mathbf{x}^{*} \leftarrow \text{None}$ ;
2 for  $\mathbf{x}'$  in  $\hat{\mathcal{G}}_{\mathcal{I}}$  do
3   Get the loss  $\mathcal{J}_{iden}(\mathbf{x}', \mathbf{x}^{adv})$  via Eq. (3);
4   Compute the gradient  $\nabla_{\mathbf{x}} \mathcal{J}_{iden}(\mathbf{x}', \mathbf{x}^{adv})$ ;
5   Generate candidate adversarial example
       $\hat{\mathbf{x}}^{adv} = \Pi_{\{\mathbf{x}^{real}, \ell_p, \epsilon\}}(\mathbf{x}^{adv} - \alpha \cdot \text{Normalize}(\nabla_{\mathbf{x}} \mathcal{J}_{iden}(\mathbf{x}', \mathbf{x}^{adv})))$ ;
6   Calculate  $g = G(\hat{\mathbf{x}}^{adv})$ ;
7   if  $g > g_{best}$  then
8      $g_{best} \leftarrow g$ ;  $\mathbf{x}^{*} \leftarrow \mathbf{x}'$ ;
9   end
10 end

```

4.3 Inner Minimization via Greedy Insertion

The target set $\hat{\mathcal{G}}_{\mathcal{I}}$ containing multiple identities offers more potential optimization directions to get better performance. Therefore, we aim to develop an optimization algorithm to solve the inner minimization problem $\min_{\mathbf{x}' \in \hat{\mathcal{G}}_{\mathcal{I}}} \mathcal{J}_{iden}(\mathbf{x}', \mathbf{x}^{adv})$, where we omit the index i in Eq. (5) for clarity. For the iterative procedure in Eq. (7) with T iterations, we need to select a representative target for each adversarial example in $\hat{\mathcal{G}}_{\mathcal{I}}$ at each iteration for updates, which belongs to a subset selection problem.

Definition 1. Let S_t denote the set of the selected targets from $\hat{\mathcal{G}}_{\mathcal{I}}$ at each iteration until the t -th iteration. Let F denote a set mapping function that outputs a gain value (larger is better) in \mathbb{R} for a set. For $\mathbf{x}' \in \hat{\mathcal{G}}_{\mathcal{I}}$, we define $\Delta(\mathbf{x}'|S_t) = F(S_t \cup \{\mathbf{x}'\}) - F(S_t)$ be the marginal gain of F at S_t given \mathbf{x}' .

Formally, as the iteration gets increasing in the iteration loop, if the marginal gain decreases monotonically, then F will belong to the family of submodular functions [36]. For a submodular problem, a greedy algorithm can be used to find an approximate solution, and it has been shown that submodularity will have a $(1 - 1/e)$ -approximation [20] for monotonely submodular functions. Although our iterative identity-protection setting is not guaranteed to be strictly submodular, the solution based on greedy insertion still plays a quite obvious role, even if submodularity is not strictly decreased [36,6]. Therefore, we adopt the greedy insertion solution as an approximately optimal solution for our multi-target problem.

By analyzing the above setting, we perform the approximate submodular optimization by greedy insertion algorithm, which calculates the gain of every object from the target set at each iteration and integrates the object with the

largest gain into current subset S_t by Definition 1 as

$$S_{t+1} = S_t \cup \{\arg \max_{\mathbf{x}' \in \hat{\mathcal{G}}_{\mathcal{I}}} \Delta(\mathbf{x}' | S_t)\}. \quad (8)$$

To achieve this, we need to define the above set mapping function F . In particular, we specify F as first generating an adversarial sample \mathbf{x}^{adv} given the targets in S_t for t iterations via Eq. (7), and then using a function G to compute a gain value by Definition 1. An appropriate gain function G should choose examples that are effective for minimizing $\mathcal{J}_{iden}(\mathbf{x}', \mathbf{x}^{adv})$ at each iteration. It is noted that G must also have positive value and a larger value indicates better performance. Based on this analysis, we design a feature-based similarity gain function as

$$G(\mathbf{x}^{adv}) = \log \left(1 + \max_{\mathbf{x}' \in \hat{\mathcal{G}}_{\mathcal{I}}} \exp(\mathcal{D}_f(\mathbf{x}^{adv}, \mathbf{x}^{real}) - \mathcal{D}_f(\mathbf{x}^{adv}, \mathbf{x}')) \right), \quad (9)$$

where the algorithm tends to select a target closer to the real image in the feature space at each iteration, which also accords with Eq. (3). The algorithm is summarized in Algorithm 1.

5 Experiments

In this section, we conduct extensive experiments in the aspect of identity protection to demonstrate the effectiveness of the proposed method. We thoroughly evaluate different properties of our method based on various state-of-the-art face recognition models under the targeted identity-protection setting.

5.1 Experimental Settings

Datasets. The experiments are constructed on the Labeled Face in the Wild (LFW) [12] and MegFace [14] datasets. In each dataset, we first select 500 different identities as the protected identities. Meanwhile, we randomly select an image from each identity as the probe image (total 500 images), and the other images for each identity are assembled to form a gallery set. We randomly select another 10 identities as \mathcal{I} . We collect their face images from a celebrity dataset named MS-Celeb-1M [10]. We select one image for each of these target identities to form $\hat{\mathcal{G}}_{\mathcal{I}}$, while the remaining images are integrated into the gallery set. Besides, by considering the open-set face identification protocol, we add additional 500 identities to the gallery set, which also accords with the realistic scenario. We hope that the protected images given by TIP-IM can confuse black-box face identification models for the purpose of identity protection.

Target models. We select sphereface [18], CosFace [30], FaceNet [25], ArcFace [3], MobileFace [2], and ResNet50 [11] as the fundamental face recognition models. Note that these models lie in various settings, including different model architectures and training objectives. For each image in the dataset, We first use MTCNN [34] to detect faces, then we align the images and crop them to 112×112 , meaning that the identity masks are executed only in the face area.

In experiments, we only use one white-box model to generate the identity masks and test the performance against the other black-box models.

Compared Methods. We investigate many privacy protection methods [26,22,5], but few attempts have been made for black-box models and targeted privacy protection. Therefore, we incorporate several baselines. The first is TIP-IM with only one single target in Eq. (5). Besides, we demonstrate the influence of different gain functions for multi-targets optimization. We denote the additional gain functions based on Eq. (9) as $G_1(x) = \log(1 + \sum_{\mathbf{x}' \in \hat{\mathcal{G}}_{\mathcal{I}}} \exp(\mathcal{D}_f(\mathbf{x}, \mathbf{x}^{real}) - \mathcal{D}_f(\mathbf{x}, \mathbf{x}')))$ and $G_2(x) = \log(1 + \min_{\mathbf{x}' \in \hat{\mathcal{G}}_{\mathcal{I}}} \exp(\mathcal{D}_f(\mathbf{x}, \mathbf{x}^{real}) - \mathcal{D}_f(\mathbf{x}, \mathbf{x}')))$, which are named TIP-IM-G1 and TIP-TM-G2. TIP-IM-G1 promotes adversarial samples to be updated towards the mean center of target identities in the feature space, whereas TIP-IM-G2 seeks for the farthest target with current object constantly. Moreover, we denote TIP-IM-Rand as a random search method for solving the inner minimization as a comparison. We set the number of iterations as $N = 50$, the learning rate $\alpha = 1.5$ and the size of perturbation $\epsilon = 12$ under the ℓ_∞ norm bound, which are identical for all the experiments.

Evaluation Metrics. To evaluate the **protection success rate** of identity-protection attack, we report Rank-N targeted identity success rate named Rank-N-T and untargeted identity success rate named Rank-N-UT (higher is better). Specifically, given a probe image \mathbf{x} and a gallery set \mathcal{G} with at least one image of the same identity with \mathbf{x} , meanwhile \mathcal{G} has images of target identities. The face identification algorithm ranks the distance \mathcal{D}_f for all images in the gallery to \mathbf{x} . Rank-N-T means that at least one of the top N images belongs to the target identity, whereas Rank-N-UT needs to satisfy that top N images do not have the same identity as \mathbf{x} . In this paper, we report Rank-1-T, Rank-5-T, Rank-1-UT, and Rank-5-UT. To test the **imperceptibility** of the generated protected images, we adopt the standard quantitative measures—PSNR (dB) and structural similarity (SSIM) [31], as well as MMD. For SSIM and PSNR, a larger value means better image quality, whereas a smaller MMD value indicates superior performance.

5.2 Black-box Identity Protection

In this section, we report the results on the LFW dataset. Due to the space limitation, we leave the results of MegFace in Appendix B. We generate adversarial examples against CosFace, ArcFace, MobileFace, and ResNet50 respectively, by the proposed TIP-IM. We then feed the generated adversarial examples to all face models for white-box/black-box tests, as shown in Table 4. Our algorithm achieves the best performance in terms of Rank-1-T and Rank-5-T, and outperforms other methods by a large margin. Note that the Single-Target method obtains acceptable performance against white-box models, but is completely inferior to multi-target methods against black-box models. The main reason is that more targets provide more promising directions, making generated adversarial examples more effective for black-box models. Therefore, the adversarial examples from multi-targets are essential in exploring identity protection tasks.

	Attack	CosFace		ArcFace		MobileFace		ResNet50		SphereFace		FaceNet	
		R1-T	R5-T	R1-T	R5-T	R1-T	R5-T	R1-T	R5-T	R1-T	R5-T	R1-T	R5-T
CosFace	Single-Target	45.8*	70.2*	5.8	25.6	7.6	35.3	6.0	29.8	10.2	32.0	6.4	23.2
	TIP-IM-Rand	7.0*	21.6*	6.0	26.4	12.0	42.8	9.0	34.0	9.2	21.4	8.6	27.2
	TIP-IM-G1	8.2*	26.6*	7.8	31.6	14.4	44.4	11.6	41.0	8.8	26.0	8.0	30.4
	TIP-IM-G2	6.6*	19.4*	7.8	21.8	13.2	38.0	9.8	34.8	7.0	23.4	6.4	24.4
	TIP-IM	61.6*	85.2*	31.0	62.6	48.8	77.8	39.8	67.2	22.6	48.2	33.0	57.0
ArcFace	Single-Target	2.6	11.0	94.8*	97.6*	16.8	48.0	10.8	34.8	4.2	15.6	4.4	19.0
	TIP-IM-Rand	2.0	11.2	34.8*	68.2*	18.8	53.6	15.8	46.0	3.8	18.4	9.6	33.6
	TIP-IM-G1	3.8	13.0	59.4*	84.6*	36.8	66.0	28.8	57.6	6.6	21.4	11.8	35.4
	TIP-IM-G2	1.6	8.6	39.0*	70.6*	22.8	55.4	17.2	47.4	5.8	20.0	9.0	30.4
	TIP-IM	11.4	31.0	97.2*	98.8*	69.8	90.6	56.0	80.6	13.2	32.0	32.8	56.2
MobileFace	Single-Target	1.2	5.2	9.4	28.8	96.6*	98.4*	28.8	63.2	6.2	19.2	4.8	20.6
	TIP-IM-Rand	2.0	11.0	10.6	30.2	40.2*	73.2*	18.6	49.4	6.8	22.2	9.8	27.0
	TIP-IM-G1	3.6	12.4	14.8	41.8	53.0*	83.4*	21.8	53.6	5.8	25.6	12.2	29.6
	TIP-IM-G2	1.4	11.2	8.4	32.6	30.2*	68.4*	16.8	44.2	5.4	19.8	8.0	22.2
	TIP-IM	12.4	31.2	44.0	68.2	96.6*	99.2*	62.8	85.8	12.6	29.8	28.8	46.2
ResNet50	Single-Target	2.0	6.6	7.0	26.4	26.6	57.2	31.4*	65.0*	9.2	24.2	6.8	22.8
	TIP-IM-Rand	1.8	8.8	14.2	37.6	22.4	52.6	31.4*	65.0*	5.2	16.8	9.4	29.2
	TIP-IM-G1	2.4	12.0	13.2	37.14	26.8	58.6	41.6*	73.4*	6.8	21.0	9.2	27.2
	TIP-IM-G2	1.6	9.8	8.8	31.2	20.6	49.0	21.4*	56.8*	3.2	16.8	7.8	27.2
	TIP-IM	10.8	26.2	34.2	56.8	62.4	83.4	95.6*	98.2*	11.4	25.6	23.2	40.0

Table 2. Rank-1-T and Rank-5-T (%) of black-box privacy protection against CosFace, SphereFace, FaceNet, ArcFace, MobileFace, and ResNet. * indicates white-box results.

	Metric	$\gamma=0$	$\gamma=0.2$	$\gamma=0.4$	$\gamma=0.6$
CosFace	PSNR	25.26	25.34	25.60	26.73
	SSIM	0.6497	0.6562	0.6764	0.7389
	MMD	0.7569	0.7567	0.7563	0.7541
ArcFace	PSNR	25.26	25.59	26.08	27.63
	SSIM	0.6520	0.6690	0.6986	0.7817
	MMD	0.7567	0.7562	0.7554	0.7518
MobileFace	PSNR	25.24	25.18	25.72	27.19
	SSIM	0.6490	0.6523	0.6828	0.7533
	MMD	0.7567	0.7568	0.7559	0.7525
ResNet50	PSNR	25.14	25.26	25.74	27.21
	SSIM	0.6507	0.6595	0.6897	0.760
	MMD	0.7570	0.7567	0.7558	0.7525

Table 3. The average PSNR (db), SSIM, and MMD of the protected images generated by TIP-IM with different γ for each face model.

We report the results of Rank-5-UT in Appendix A, which demonstrates that it can still maintain an average accuracy over 70% for black-box models.

Ablation Study. As shown in Table 4, it can be also observed that different gain functions extremely influence the performance, which means that an appropriate gain function is important to achieve good black-box performance. Among different gain functions, the original one defined in Eq. (9) achieves the best performance, meaning that an effective method is that we select the closest target in the feature space as the update direction. Note that the adversarial examples generated against MobileFace have excellent transferability to the other black-box models. This observation might be explained that the simple convolutional structure of networks can obtain more universal features.

Comparison experiments about target images. We test the performance of different numbers of targets in Appendix D, which implies that appropriate increases in the number of targets is beneficial to performance improve-

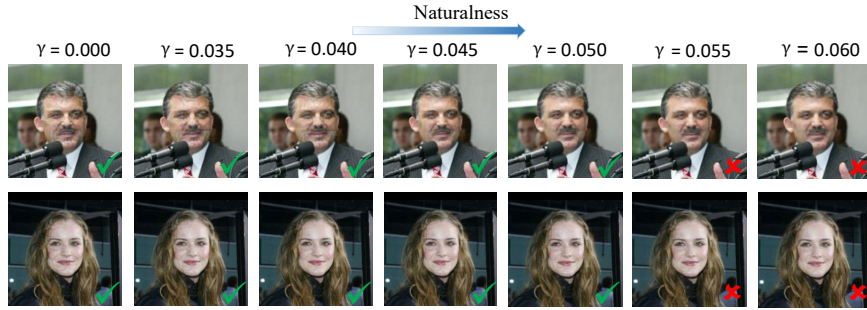


Fig. 3. Experiments on how different γ affects the performance of adversarial samples. Green hook refers to successful targeted identity protection while red hook refers to failure, which also implies a trade-off on effectiveness and naturalness.

ment against black-box models. We specify some *generated* images from StyleGAN [13] as target images. The results in Appendix D show that our algorithm still has excellent black-box performance of identity protection. In practical applications, we can arbitrarily specify the available and authorized target identity set or generated face images, and our algorithm is applicable to any target set.

5.3 Naturalness

To examine whether our algorithm is able to control the naturalness of adversarial examples in the process of generating the samples, we perform experiments with different coefficient γ . Table 3 shows the evaluation results of different face identification models (including CosFace, ArcFace, MobileFace, and ResNet50) in terms of three different metrics—PSNR, SSIM, and MMD. As the coefficient γ increases, the visual quality of the generated images is getting better based on different metrics, which is also consistent with the example in Fig. 3. Therefore, conditioned on different γ , we can control the degree of the generated adversarial images.

5.4 Trade-off between Effectiveness and Naturalness

Apart from quantitative measures, we also performed naturalness manipulation for different coefficient γ dynamically, as illustrated in Fig. 3. It can be seen that the image looks more natural as the γ increases, whereas to a certain extent identity protection tends to fail, meaning that there exists a trade-off between black-box obfuscation effectiveness and naturalness. Therefore, we also perform a more comprehensive evaluation on all given identity recognition models in Fig. 4. We study the effect of different coefficients γ on the success rate of attacks. Four face identification models including CosFace, ArcFace, MobileFace, and Resnet50 have similar trends. As the coefficient γ increases, naturalness assessment indicators SSIM are also rising, but there exists a general downward trend for Rank-1-T accuracy. Notably that Rank-1-T rises first and then falls, meaning that appropriate γ can make transferability more effective. In practical

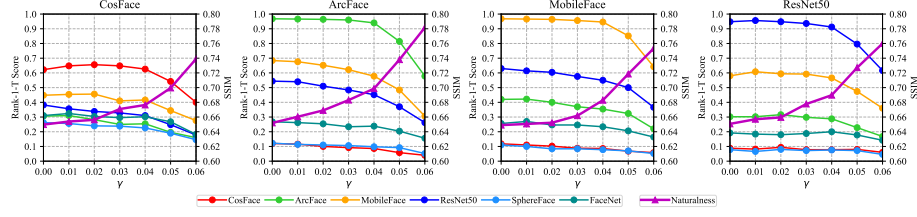


Fig. 4. Rank-1-T score and SSIM of adversarial examples generated by TIP-IM with different γ against CosFace, SphereFace, FaceNet, ArcFace, MobileFace, and ResNet50.

applications, users can adjust γ to control stronger obfuscation performance (effectiveness) or visual quality (naturalness).

5.5 Privacy Protection on a Real-World Application

In this section, we apply our proposed TIP-IM to test the privacy protection performance on a commercial face search API available at Tencent AI Open Platform³. The working mechanism is completely unknown for us. To simulate the privacy data scenario, we use the same gallery set with over 6,000 images and 1,000 identities (including 10 target identities) described above. We choose 20 probe faces from above probe set to execute face search based on similarity ranking in this platform. All 20 probe faces can be identified at rank1. Then we generate corresponding protected images from probe faces to execute face search. For return rankings there exists 6 target identities in rank1 and 16 in rank5. Note that Faces with the same identity also show a decreasing similarity in different degrees, which also illustrates the effectiveness for black-box face system, and two examples are shown in Fig. 5.



Fig. 5. Examples of privacy protection on the real-world face recognition API. We separately use real and protected faces by TIP-IM as probes to do face search and show top three results by similarity. Blue boxes represent the faces with same identities as probe faces and green boxes imply the faces belonging to targeted identities. Similarity scores with probe face are marked in yellow.

³ <https://ai.qq.com/product/face.shtml>

6 Conclusion

In this paper, we studied the problem of identity protection by simulating realistic identification systems in the social media. A practical setting called targeted identity-protection and a novel targeted identity-protection iterative method (TIP-IM) are introduced, which enable users to protect their private information from being exposed by the unauthorized identification systems while not affecting the user experience in social media. Extensive experiments based on the state-of-the-art face recognition models demonstrate that our algorithm can effectively alleviate the identity leakage of face images.

A Additional Evaluation Results on LFW.

We report the results of Rank-1-UT and Rank-5-UT on LFW dataset in Tab. 4. Different multi-target methods are not much different in the aspect of untargeted ranking, yet excel the single-target method.

	Attack	CosFace		ArcFace		MobileFace		ResNet50		SphereFace		FaceNet	
		R1-U	R5-U	R1-U	R5-U	R1-U	R5-U	R1-U	R5-U	R1-U	R5-U	R1-U	R5-U
CosFace	Single-Target	95.0*	93.4*	44.8	30.8	56.2	45.0	46.6	37.8	88.8	81.2	68.0	52.8
	TIP-IM-Rand	96.6*	94.6*	52.8	42.4	65.0	52.4	55.0	45.8	92.2	88.2	78.2	63.8
	TIP-IM-G1	95.8*	95.4*	55.8	42.8	66.0	54.8	57.2	46.6	91.4	86.2	75.6	63.8
	TIP-IM-G2	95.4*	95.5*	54.6	43.0	65.6	53.0	57.2	46.2	91.6	86.2	76.0	66.0
	TIP-IM	96.6*	95.4*	54.2	39.4	64.8	51.2	57.2	44.2	89.0	84.0	73.6	61.2
ArcFace	Single-Target	74.2	62.8	95.8*	91.8*	67.6	58.2	58.2	48.0	79.6	68.2	67.4	53.6
	TIP-IM-Rand	80.0	72.2	96.0*	93.6*	73.6	65.2	64.8	54.2	82.8	73.0	73.0	60.0
	TIP-IM-G1	82.0	72.8	96.0*	95.2*	79.0	70.0	68.2	59.0	85.2	76.6	73.4	63.4
	TIP-IM-G2	84.0	73.0	95.6*	93.4*	73.0	65.2	63.4	55.4	83.8	74.0	73.6	60.8
	TIP-IM	74.0	63.8	97.4*	96.4*	79.4	68.8	70.4	56.8	78.6	68.4	70.0	57.8
MobileFace	Single-Target	75.6	62.2	60.2	45.4	96.6*	92.0*	72.2	59.0	80.0	69.6	68.4	53.6
	TIP-IM-Rand	79.4	67.0	67.2	55.4	95.4*	93.6*	77.6	68.4	83.2	73.2	74.6	60.6
	TIP-IM-G1	80.0	67.8	67.4	58.0	95.0*	93.6*	80.8	73.8	84.4	74.6	77.0	62.0
	TIP-IM-G2	79.4	68.2	66.4	57.4	95.2*	94.6*	80.0	71.4	84.4	74.0	77.6	60.4
	TIP-IM	74.4	61.2	68.6	52.8	96.6*	94.8*	81.4	71.2	78.6	65.0	75.0	58.6
ResNet50	Single-Target	77.6	64.2	61.8	50.4	80.6	72.2	95.4*	91.6*	80.4	65.8	69.0	53.2
	TIP-IM-Rand	83.0	71.8	73.2	59.0	84.8	78.2	95.0*	93.8*	83.2	74.4	79.4	63.8
	TIP-IM-G1	82.8	72.4	70.0	59.6	87.0	81.8	95.8*	94.8*	85.8	75.0	78.8	65.0
	TIP-IM-G2	83.6	73.0	71.6	58.4	85.2	77.4	95.4*	92.8*	84.0	74.2	77.4	65.4
	TIP-IM	77.0	65.8	68.0	54.6	85.4	77.4	96.8*	94.6*	77.6	65.4	72.6	60.8

Table 4. Rank-1-UT and Rank-5-UT (%) of black-box attacks against CosFace, SphereFace, FaceNet, ArcFace, MobileFace, ResNet. * indicates white-box attacks.

B Evaluation Results on MegFace.

We report the results on the MegFace dataset in Tab. 5. Compared with LFW, MegFace has more gallery images, resulting in more difficult identity protection on the whole.

	Attack	CosFace		ArcFace		MobileFace		ResNet50		SphereFace		FaceNet	
		R1-T	R5-T	R1-T	R5-T	R1-T	R5-T	R1-T	R5-T	R1-T	R5-T	R1-T	R5-T
CosFace	Single-target	9.0*	20.8*	3.6	16.0	7.4	24.6	4.8	19.0	1.4	11.0	4.8	14.8
	TIP-IM	39.0*	61.2*	30.4	53.2	42.6	65.8	34.6	55.4	7.8	24.4	25.0	48.6
ArcFace	Single-target	1.4	7.6	92.0*	97.0*	11.6	36.0	8.0	23.4	1.6	7.6	3.4	13.4
	TIP-IM	8.6	22.4	97.0*	98.2*	60.2	81.2	51.0	67.8	4.6	16.4	24.8	43.0
MobileFace	Single-target	2.0	9.2	5.8	19.4	94.8*	96.4*	18.6	42.0	2.8	9.6	4.0	14.2
	TIP-IM	8.0	19.4	37.0	57.6	97.2*	97.6*	52.8	73.2	3.2	12.4	18.0	34.8
ResNet50	Single-target	3.2	9.2	7.8	19.0	15.2	44.2	91.4*	95.4*	2.6	13.0	4.8	16.8
	TIP-IM	7.2	22.0	29.0	44.8	56.6	76.8	92.2*	97.0*	2.4	13.8	18.4	32.0

Table 5. Rank-1-T and Rank-5-T (%) of black-box attacks against CosFace, SphereFace, FaceNet, ArcFace, MobileFace, ResNet on MegFace. * indicates white-box attacks.

C Batch Analysis on MMD Optimization.

Tab. 6 shows results on different batch sizes w.r.t naturalness. It can be seen that the evaluation of visual quality becomes stable as the batch size exceeds 50. We set batch size as 50 in this paper. For single image crafting, we have two choices. The first one is self augmentation including rotation, projective, brightness and transformations; The second one is collecting some irrelevant images to form a batch just for optimal results in the phase of MMD optimization.

	10	20	30	40	50	60	70	80	90
SSIM	0.8518	0.8392	0.7592	0.7021	0.6759	0.6765	0.6633	0.6649	0.6674
PSNR(db)	28.71	28.55	26.95	26.02	25.55	25.63	25.40	25.50	25.54

Table 6. The mean PSNR (db) and SSIM for different batch sizes based on CosFace.

D Comparison Experiments about Target Images.

Different numbers of targets. As illustrated in Fig. 6, we study the effect of different numbers on the black-box identity protection. The curve first rises and finally approaches the steady. Therefore, appropriate increases in the number of targets is beneficial to performance improvement against black-box models.

Generated images as targets. To further verify that our algorithm does not depend on the selection of targets, we specify some generated images from StyleGAN [13] as target images, which is illustrated as Fig. 7. We use these generated images as target images and set the same other setting with above experiments. Tab. 7 shows Rank-1-T, Rand-1-UT, Rank-5-T and Rank-5-UT of black-box attacks against CosFace, SphereFace, FaceNet, ArcFace, MobileFace and ResNet. The results show that our algorithm still has excellent black-box performance of identity protection. In practical applications, we can arbitrarily

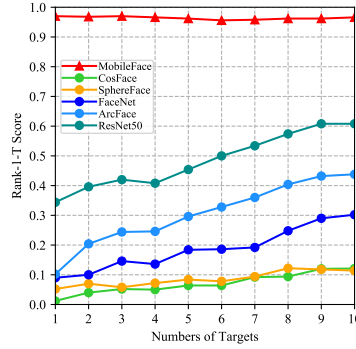


Fig. 6. The perturbation vs. numbers of targets curve of face identification models against black-box identity protection. *MobileFace* is a surrogate white-box model.

specify the available and authorised target identity set or some generated facial images, and our algorithm is applicable to any target set.



Fig. 7. Examples of some generated images from StyleGAN [13].

	CosFace	ArcFace	MobileFace	ResNet50	SphereFace	FaceNet
Rank-1-T	49.6	12.2	32.4	29.2	27.4	28.2
Rank-5-T	70.0	30.4	52.2	54.8	56.4	53.8
Rank-1-UT	95.0	89.0	73.8	49.6	60.8	54.2
Rank-5-UT	93.6	82.0	55.8	31.6	41.8	34.8

Table 7. Results of black-box attacks against CosFace, SphereFace, FaceNet, ArcFace, MobileFace, ResNet when treating the *generated* images as the target images. CosFace is used as substitute model.

References

1. Borgwardt, K.M., Gretton, A., Rasch, M.J., Kriegel, H.P., Schölkopf, B., Smola, A.J.: Integrating structured biological data by kernel maximum mean discrepancy. *Bioinformatics* **22**(14), e49–e57 (2006)
2. Chen, S., Liu, Y., Gao, X., Han, Z.: Mobilefacenets: Efficient cnns for accurate real-time face verification on mobile devices. In: *Chinese Conference on Biometric Recognition*. pp. 428–438. Springer (2018)

3. Deng, J., Guo, J., Xue, N., Zafeiriou, S.: Arcface: Additive angular margin loss for deep face recognition. In: *Proceedings of the IEEE Conference on Computer Vision and Pattern Recognition*. pp. 4690–4699 (2019)
4. Dong, Y., Liao, F., Pang, T., Su, H., Zhu, J., Hu, X., Li, J.: Boosting adversarial attacks with momentum. In: *Proceedings of the IEEE Conference on Computer Vision and Pattern Recognition (CVPR)* (2018)
5. Dong, Y., Su, H., Wu, B., Li, Z., Liu, W., Zhang, T., Zhu, J.: Efficient decision-based black-box adversarial attacks on face recognition. In: *Proceedings of the IEEE Conference on Computer Vision and Pattern Recognition (CVPR)* (2019)
6. Feige, U., Mirrokni, V.S., Vondrák, J.: Maximizing non-monotone submodular functions. *SIAM Journal on Computing* **40**(4), 1133–1153 (2011)
7. Gafni, O., Wolf, L., Taigman, Y.: Live face de-identification in video. In: *Proceedings of the IEEE International Conference on Computer Vision*. pp. 9378–9387 (2019)
8. Goodfellow, I., Pouget-Abadie, J., Mirza, M., Xu, B., Warde-Farley, D., Ozair, S., Courville, A., Bengio, Y.: Generative adversarial nets. In: *Advances in neural information processing systems*. pp. 2672–2680 (2014)
9. Goodfellow, I.J., Shlens, J., Szegedy, C.: Explaining and harnessing adversarial examples. In: *International Conference on Learning Representations (ICLR)* (2015)
10. Guo, Y., Zhang, L., Hu, Y., He, X., Gao, J.: Ms-celeb-1m: A dataset and benchmark for large-scale face recognition. In: *European Conference on Computer Vision*. pp. 87–102. Springer (2016)
11. He, K., Zhang, X., Ren, S., Sun, J.: Identity mappings in deep residual networks. In: *European Conference on Computer Vision (ECCV)*. pp. 630–645. Springer (2016)
12. Huang, G.B., Mattar, M., Berg, T., Learned-Miller, E.: Labeled faces in the wild: A database for studying face recognition in unconstrained environments (2008)
13. Karras, T., Laine, S., Aittala, M., Hellsten, J., Lehtinen, J., Aila, T.: Analyzing and improving the image quality of StyleGAN
14. Kemelmacher-Shlizerman, I., Seitz, S.M., Miller, D., Brossard, E.: The megaface benchmark: 1 million faces for recognition at scale. In: *Proceedings of the IEEE Conference on Computer Vision and Pattern Recognition*. pp. 4873–4882 (2016)
15. Kurakin, A., Goodfellow, I., Bengio, S.: Adversarial examples in the physical world. In: *International Conference on Learning Representations (ICLR) Workshops* (2017)
16. Larson, M., Liu, Z., Brugman, S., Zhao, Z.: Pixel privacy: increasing image appeal while blocking automatic inference of sensitive scene information (2018)
17. Li, T., Lin, L.: Anonymousnet: Natural face de-identification with measurable privacy. In: *Proceedings of the IEEE Conference on Computer Vision and Pattern Recognition Workshops*. pp. 0–0 (2019)
18. Liu, W., Wen, Y., Yu, Z., Li, M., Raj, B., Song, L.: Sphreface: Deep hypersphere embedding for face recognition. In: *Proceedings of the IEEE conference on computer vision and pattern recognition*. pp. 212–220 (2017)
19. McPherson, R., Shokri, R., Shmatikov, V.: Defeating image obfuscation with deep learning. *arXiv preprint arXiv:1609.00408* (2016)
20. Nemhauser, G.L., Wolsey, L.A., Fisher, M.L.: An analysis of approximations for maximizing submodular set functions. *Mathematical programming* **14**(1), 265–294 (1978)
21. Oh, S.J., Benenson, R., Fritz, M., Schiele, B.: Faceless person recognition: Privacy implications in social media. In: *European Conference on Computer Vision*. pp. 19–35. Springer (2016)

22. Oh, S.J., Fritz, M., Schiele, B.: Adversarial image perturbation for privacy protection a game theory perspective. In: 2017 IEEE International Conference on Computer Vision (ICCV). pp. 1491–1500. IEEE (2017)
23. Papernot, N., McDaniel, P., Goodfellow, I., Jha, S., Celik, Z.B., Swami, A.: Practical black-box attacks against deep learning systems using adversarial examples. arXiv preprint arXiv:1602.02697 (2016)
24. Ribaric, S., Ariyaeinia, A., Pavesic, N.: De-identification for privacy protection in multimedia content: A survey. *Signal Processing: Image Communication* **47**, 131–151 (2016)
25. Schroff, F., Kalenichenko, D., Philbin, J.: Facenet: A unified embedding for face recognition and clustering. In: Proceedings of the IEEE conference on computer vision and pattern recognition. pp. 815–823 (2015)
26. Sharif, M., Bhagavatula, S., Bauer, L., Reiter, M.K.: Accessorize to a crime: Real and stealthy attacks on state-of-the-art face recognition. In: ACM Sigsac Conference on Computer and Communications Security. pp. 1528–1540 (2016)
27. Sun, Q., Ma, L., Joon Oh, S., Van Gool, L., Schiele, B., Fritz, M.: Natural and effective obfuscation by head inpainting. In: Proceedings of the IEEE Conference on Computer Vision and Pattern Recognition. pp. 5050–5059 (2018)
28. Sun, Q., Tewari, A., Xu, W., Fritz, M., Theobalt, C., Schiele, B.: A hybrid model for identity obfuscation by face replacement. In: Proceedings of the European Conference on Computer Vision (ECCV). pp. 553–569 (2018)
29. Szegedy, C., Zaremba, W., Sutskever, I., Bruna, J., Erhan, D., Goodfellow, I., Fergus, R.: Intriguing properties of neural networks. In: International Conference on Learning Representations (ICLR) (2014)
30. Wang, H., Wang, Y., Zhou, Z., Ji, X., Gong, D., Zhou, J., Li, Z., Liu, W.: Cosface: Large margin cosine loss for deep face recognition. In: Proceedings of the IEEE Conference on Computer Vision and Pattern Recognition. pp. 5265–5274 (2018)
31. Wang, Z., Bovik, A.C., Sheikh, H.R., Simoncelli, E.P., et al.: Image quality assessment: from error visibility to structural similarity. *IEEE transactions on image processing* **13**(4), 600–612 (2004)
32. Wilber, M.J., Shmatikov, V., Belongie, S.: Can we still avoid automatic face detection? In: 2016 IEEE Winter Conference on Applications of Computer Vision (WACV). pp. 1–9. IEEE (2016)
33. Wu, Y., Yang, F., Ling, H.: Privacy-protective-gan for face de-identification. arXiv preprint arXiv:1806.08906 (2018)
34. Zhang, K., Zhang, Z., Li, Z., Qiao, Y.: Joint face detection and alignment using multitask cascaded convolutional networks. *IEEE Signal Processing Letters* **23**(10), 1499–1503 (2016)
35. Zhao, Z., Dua, D., Singh, S.: Generating natural adversarial examples. In: International Conference on Learning Representations (ICLR) (2018)
36. Zhou, Y., Spanos, C.J.: Causal meets submodular: Subset selection with directed information. In: Advances In Neural Information Processing Systems. pp. 2649–2657 (2016)